# Postflight Evaluation of the Shuttle Guidance, Navigation, and Control During Powered-Ascent Flight Phase

LeRoy M. Olson*
*McDonnell Douglas Technical Services Company, Houston, Texas*
and
John W. Sunkel†
*NASA Johnson Space Center, Houston, Texas*

**An overview of the ascent trajectory and the guidance, navigation, and control system design is followed by a summary of flight test results for the ascent phase of the first Space Shuttle flight. The most notable variance from nominal preflight predictions was the lofted trajectory observed in first stage due to an unanticipated shift in pitch aerodynamic characteristics from those predicted by wind-tunnel tests. The guidance, navigation, and control systems performed as expected throughout powered flight. Following a discussion of the software constants changed for flight 2 to provide an adequate performance margin, a summary of test results from the second and third shuttle flights is presented. Vehicle trajectory response and system behavior were very similar to the first flight. Ascent aerodynamic characteristics extracted from the first two test flights were included in the data base used to design the first-stage steering and pitch trim profiles for the third flight.**

## Introduction

LAUNCH of the STS-1 from launch complex 39A at Cape Canaveral, Fla., on April 12, 1981, marked the beginning of a nearly flawless first Shuttle test flight. Data collected on vehicle subsystem performance and operating environments will be used to allow incremental expansion of the flight envelope in subsequent test flights, leading ultimately to verification of the fully operational Shuttle.

First flight came after more than a decade of design, development, and verification activities leading to certification of a rather complex vehicle avionics system. The quad-redundant, fly-by-wire digital guidance, navigation, and control (GN&C) system provides automatic steering for ascent but also includes a man-in-the-loop capability that may be required in contingency abort situations. Four general-purpose computers (GPC) each perform identical computations in a synchronized manner, using inputs from redudant sensors. Thrust vector control (TVC) and aerosurface actuators thus receive four parallel commands that are force-summed at the power valve.

Since the avionics system is designed to be two-fault tolerant (fail operational/fail safe) redundancy management is an integral part of the GN&C system. Redundant sensor inputs are sampled at the user rate (25 Hz for rate gyros and accelerometers) and the middle value is selected for use by the flight control system. Fault detection and isolation algorithms are processed at lower rates and once a sensor is declared failed, the high-rate selection process is moded accordingly and fault annunciation is displayed to the crew and telemetered to the ground. Since the GPCs do not have adequate memory capability for the entire mission profile, the software has been structured into several memory loads, including ground checkout, ascent, on-orbit, on-orbit checkout, and entry. These load blocks are stored on redundant mass memory units and GPC memory is reloaded at appropriate points along the mission profile. The ascent load provides GN&C software for use throughout the terminal count starting at $t-20$ min through orbit circularization. A portion of the GPC memory is preserved across the phase transitions, which includes the operating system software, state vector, sensor and effector configuration, and failure status and initialization data.

## Ascent Trajectory Description

The ascent phase begins with ignition of the solid rocket boosters (SRB) and terminates at orbit insertion or at landing at the Kennedy Space Center in the case of a return to landing site (RTLS) abort that would be required with an Orbiter engine failure early in powered flight. Three subphases of a normal ascent including stage 1 from liftoff to SRB separation, stage 2 from separation to main engine cutoff (MECO), and a coasting phase that includes two orbital maneuvering system (OMS) engine burns for orbital circularization.

The Space Shuttle is launched from a vertical position with the tail south on the launch pad. Following a short vertical rise to clear the launch tower, a three-axis maneuver is performed to orient the vehicle to the desired flight azimuth. A programmed pitch rate continues for the remainder of first-stage flight until SRB staging when a constant attitude is maintained for several seconds to minimize the probability of recontact with the spent solids. During ascent the Shuttle flies in a "tail-down" attitude so that the Orbiter thrust, inclined 12 deg to the vehicle centerline, lifts the vehicle trajectory at zero angle of attack. Dynamic pressure $\bar{Q}$ reaches its maximum value about 50 s after liftoff and follows a plateau for approximately 30 s before decreasing at higher altitude. The characteristic $\bar{Q}$ profile is achieved by appropriately shaping the stage 1 pitch command profile and throttling the main engines back to near their minimum power level (65%) through the high $\bar{Q}$ region. Nominal $\bar{Q}$ maximum was designed to be less than 600 lb/ft$^2$ for STS-1 to minimize aerodynamic loads and will be increased incrementally through the remainder of the flight test program. Orbiter aerodynamic surfaces are not used for control during ascent but the elevons follow an open-loop position profile in the first stage to avoid excessive hinge moment and wing bending and torsion loads. A closed-loop elevon load relief feature is available to command the elevons away from the open-loop

Presented as Paper 82-1554 at the AIAA Guidance and Control, Atmospheric Flight Mechanics and Astrodynamics Conference, San Diego, Calif., Aug. 9-11, 1982; submitted Aug. 9, 1982; revision received April 4, 1983. 

*Aerospace Engineer, Houston Astronautics Division.
†Aerospace Engineer, Avionics Systems Division. Member AIAA.

profile, if required, based on measured actuator differential pressure.

Approximately 6 s after SRB staging the stage 2 closed-loop guidance is initiated to steer the vehicle to the desired MECO target conditions on velocity, flight path angle, altitude, and orbital plane. Late in stage 2, the guidance commands throttling of the main engines to limit vehicle acceleration to 3 g. MECO occurs at an altitude of approximately 385,000 ft at an inertial velocity of 25,668 ft/s. At this point, the vehicle is still on a suborbital trajectory to allow disposal of the external tank (ET) in the Indian Ocean.

Eighteen seconds after MECO, the Orbiter is separated from the ET and the coast-phase transitional autopilot (Trans DAP) commands the downfiring reaction control system (RCS) thrusters on to provide a vertical velocity increment of 1 ft/s, providing comfortable clearance from the separated tank. At MECO plus 2 min, a short OMS burn (of approximately 2 min duration) is performed to raise both apogee and perigee. Thirty minutes later, a second OMS burn raises perigee to circularize at the desired orbital altitude. During the first OMS burn, residual propellant in the main engines and manifolds is dumped overboard and the main engines are commanded to a stowed position prior to deactivation of the Orbiter hydraulic systems.

## Ascent GN&C Overview

A simplified GN&C software overview is shown in Fig. 1. The sensors used for ascent include rate gyros, normal and lateral accelerometers, and inertial measurement units (IMU). GPC computations of flight control inner-loop errors are performed at 25 Hz and transport delay is kept to less than 20 ms to preserve an adequate closed-loop autopilot phase margin. Less time-critical navigation and guidance functions are processed at lower sample rates to keep the overall computing demand within the capabilities of the GPC.

The ascent navigation function uses selected IMU data and a model of the Earth's gravitational acceleration to maintain a current estimate of the Shuttle state vector. State initialization occurs at $t-8$ s and a precise state computation is calculated approximately every 4 s. IMU accelerometers are sampled at a 1 Hz rate and higher rate user demands are fulfilled by a propagation algorithm so that a velocity estimate is available for guidance at 6.25 Hz. During the coast phase following MECO, the IMU-sensed acceleration is not used if it is below a noise threshold and an atmospheric drag model is used instead. Also, a more accurate model of the Earth's gravity is used by including higher-order terms in addition to those used in powered flight.

First-stage guidance computations are processed at 6.25 Hz and consist of table look-up of pitch, yaw and roll attitudes, and main engine throttle commands as a function of navigation relative velocity. Velocity is used as the independent variable to provide a pitch profile that produces a desired angle-of-attack vs Mach number relationship dictated by the aerodynamic loads requirements in the high $\bar{Q}$ region. Alternate pitch tables provide the necessary steering changes required for loss of a main engine in the first stage.

Closed-loop stage 2 guidance consists of equations that cyclically compute the difference between the targeted MECO state and the recent navigated state to produce a velocity and range to go to MECO. Stage 2 guidance is processed at 0.5 Hz and consists of three major subtasks: predictor, corrector, and steering parameter computations. A constant thrust is assumed early in second stage and constant 3 g acceleration in the later portion. Stage 2 guidance provides desired thrusting direction and thrust turning rate information to the flight control system and issues throttle commands to the main engines late in second stage to limit acceleration to no more than 3 g. As MECO is approached, the position constraints are released and the guidance computational rate is increased to provide an accurate velocity cutoff.

The ascent digital autopilot design is based on a conventional two-loop closure on attitude and attitude rate. A simplified software overview is shown in Fig. 2. During the high $\bar{Q}$ region of first stage, an additional loop closure on normal and lateral acceleration is used to provide structural load alleviation.[1] Attitude erros are calculated at 12.5 Hz and rate and acceleration errors at 25 Hz. Gains are scheduled against relative velocity for stage 1 and updated at 6.25 Hz as are the reference TVC trim angle, normal acceleration, and elevon schedule profiles. Gain and trim profiles for stage 2 are scheduled as a function of calculated vehicle mass provided by stage 2 guidance. The rigid-body closed-loop control frequency is slightly greater than 1.0 rad/s to provide adequate steering response to guidance commands while maintaining a sufficient propellant slosh phase margin. The oxidizer slosh mode near 3 rad/s is phase stabilized. Flexible mode compensation is provided by multiple digital filters (as high as ninth order end-to-end in stage 1). The bending modes are gain stabilized across their frequency spectrum beginning at 12 rad/s early in 1 stage and the filter coefficients are switched at transition to stage 2. A software module called RECON provides the necessary moding of TVC biases, mixing logic changes, limiters, and faders based on mission timeline events and subsystem failure status. An example of the control law signal flow topology is shown for the stage 1

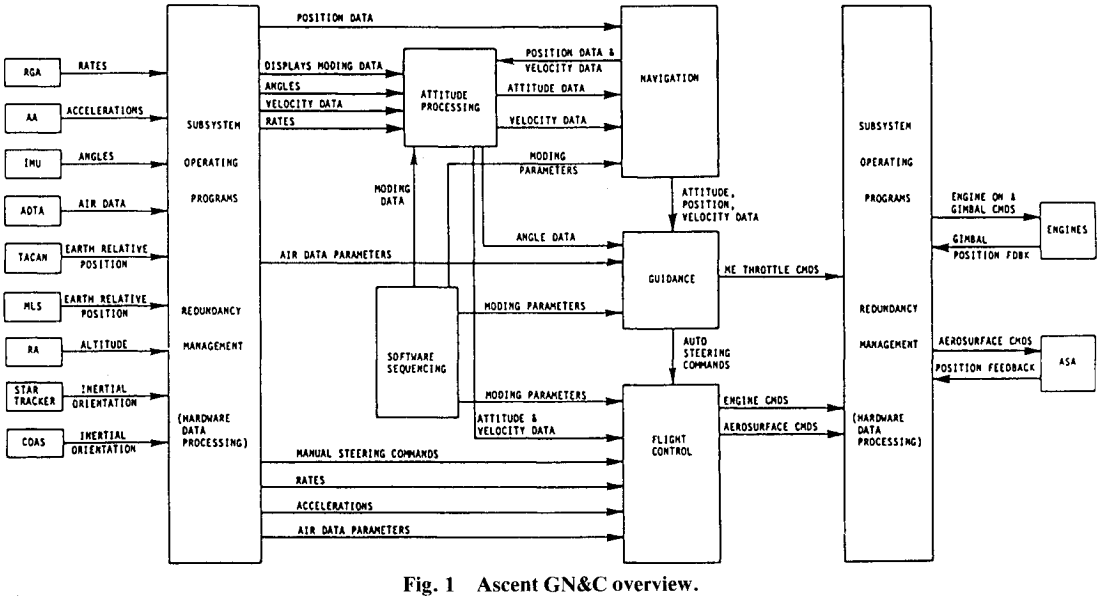


Fig. 1 Ascent GN&C overview.

pitch channel in Fig. 3. Note that a forward path integration of attitude error is used as an autotrim function to wash out the effects of sensor bias or steady-state mistrim due to thrust level imbalance or thrust vector misalignment.

## Results of First Flight

Ascent guidance and control systems performed as designed on STS-1. No significant anomalies were noted, but several interesting aspects of the dynamic behavior of the mated vehicle were observed, most notably the lofted trajectory that resulted from an unanticipated pitch attitude error during the high-dynamic-pressure region of the first-stage flight.[2,3]

Prelaunch countdown operations went smoothly and included Orbiter aerosurface and TVC actuator slew checks following hydraulic system activation at $t-4.5$ min. The SRB hydraulic systems were activated at $t-18$ s and an automatic SRB actuator slew check confirmed the health of the remainder of the actuation subsystems.

During the main propulsion system (MPS) engine thrust rise transient prior to SRB ignition, the stacked vehicle is subjected to a significant pitch bending moment. Structural response (primarily in the fundamental cantilever pitch mode) is easily noted in attitude, rate gyro, accelerometer, and ground camera data. The initial "sway-over" was slightly larger than predicted and as a result the autopilot attitude error was more than anticipated at the time of control system activation immediately following SRB ignition. The structural dynamic transient response due to SRB ignition produced sensed pitch rates of $\pm 1.0$ deg/s that damped out rather quickly (see Fig. 4). Since the autopilot bending filters provide more than 25 db of attenuation across the bending spectrum, no significant TVC actuator command transients were developed as a result of the liftoff structural response. The crew reported some initial blurring of the cockpit instrumentation that damped out by the time the tower was cleared and the roll maneuver began. The remainder of the powered flight was unmarred by instrument vibration.

Postflight reconstruction of the vehicle liftoff dynamics and autopilot response indicated near nominal facility clearance geometry. Northerly translation during the vertical rise was as expected and the absence of any discernable lateral drift confirmed the absence of any significant dispersions in SRB thrust mismatch, autopilot sensor bias, or ground winds.

Following the vertical rise, a simultaneous three-axis maneuver is programmed in stage 1 guidance to reorient the vehicle from its tail-south attitude on the pad to the head-down attitude in the desired flight azimuth. All sensor and effector data indicated nominal vehicle response and the crew reported no discernable lateral $g$ forces during the acceleration to the 10 deg/s roll rate.

Winds aloft measured prelaunch were near the statistically predicted mean of the month for which the first-stage open-loop steering profile was designed. As a result, roll and yaw attitude errors were minimal. A negative pitch attitude error began to develop after 40 s, peaked at $-5.2$ deg, and then gradually diminished toward the end of stage 1 (see Fig. 5). Postlaunch wind measurements showed little change in the in-plane pitch wind compared to the prelaunch data, indicating the attitude error was not wind induced. Post flight trajectory reconstruction efforts indicated a significant shift from wind-tunnel predictions in the pitch aero coefficients. Specifically, the differences included a more positive normal force, more negative pitch moment, and less than predicted base drag.

The incremental pitch trim required of the TVC peaked at approximately $9\times10^6$ ft-lb. As a result of the aerodynamically induced steady-state attitude error, the first-stage trajectory was lofted significantly. A comparison of flight with predicted state conditions at SRB staging is shown in Table 1.

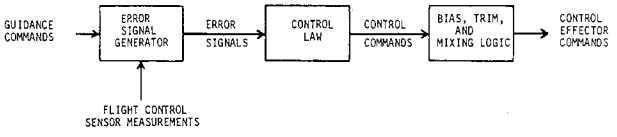


**Fig. 2 Simplifed flight control software overview.**

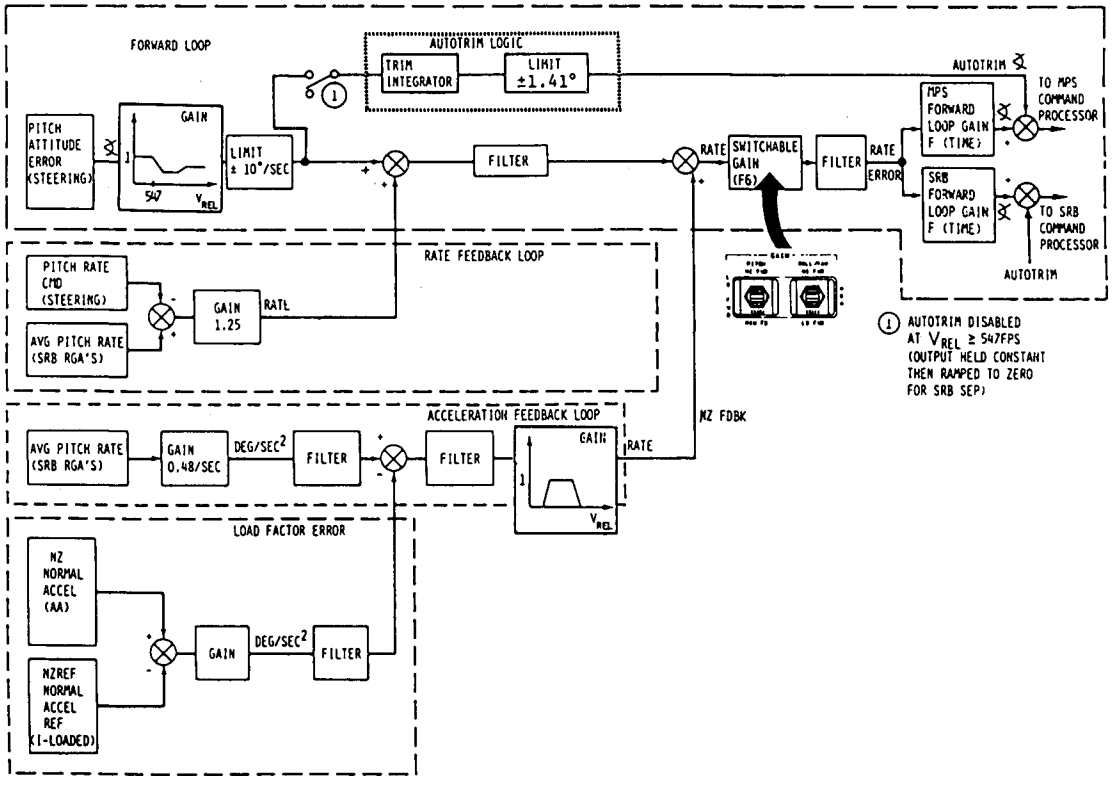


**Fig. 3 First stage pitch loop.**

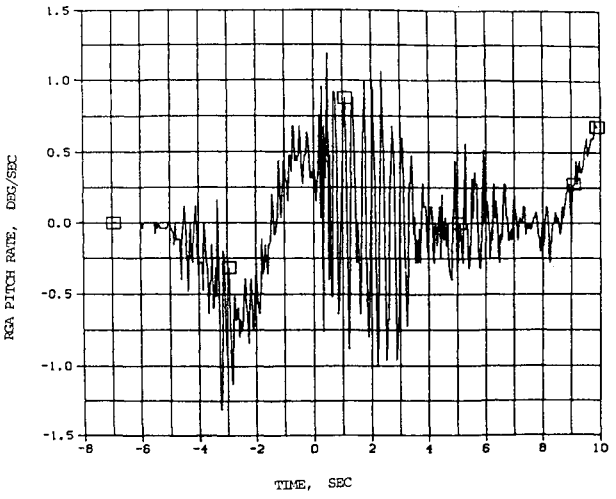


Fig. 4 STS-1 sensed pitch rate at liftoff.

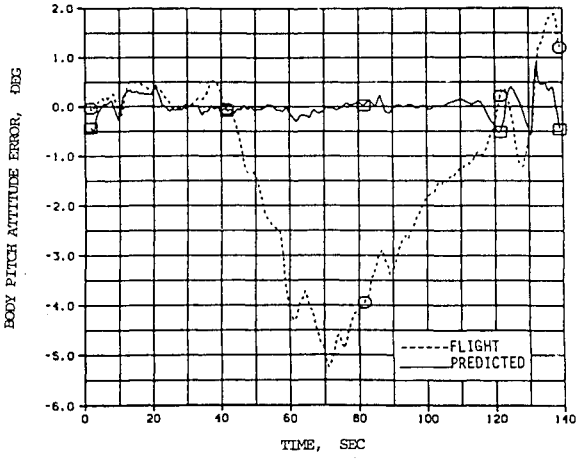


Fig. 5 STS-1 pitch attitude error.

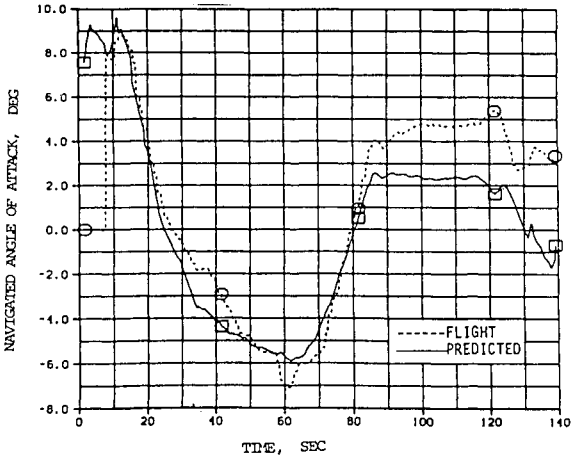


Fig. 6 STS-1 navigated angle of attack.

Table 1 SRB staging conditions

| Condition | Predicted | STS-1 | Difference |
|---|---|---|---|
| Time, | 131.68 | 130.82 | −0.86 |
| Altitude, ft | 164,736 | 173,957 | +9221 |
| Relative velocity, ft/s | 4178.56 | 4110 | −68.56 |
| Inertial velocity, ft/s | 5216.77 | 5127 | 89.8 |
| Inertial flight path angle, deg | 26.13 | 28.73 | +2.60 |

Although the pitch attitude error was rather large (the crew's ADI needle was saturated at 5 deg for more than 20 s), the rate of error buildup was gradual and the vehicle angle of attack did not deviate significantly from the predicted profile in the critical region near Mach 1 (see Fig. 6).

The trajectory design philosophy for early Shuttle flights included a constraint on maximum dynamic pressure which was 620 lb/ft$^2$ for STS-1. Maximum navigated $\bar{Q}$ was 615 lb/ft$^2$ but the actual $\bar{Q}$ including wind effects is now projected as 606 lb/ft$^2$ (see Fig. 7). Note that as a result of the lofting the flight dynamic pressure during the latter part of stage 1 was less than preflight predictions.

There was evidence of Orbiter thrust vector misalignment in stage 2 based on an examination of the attitude error histories. The thrust was expected to deflect to some extent under load, and flight data indicate somewhat larger misalignment than predicted. The autotrim function in the autopilot gradually washed out the steady-state attitude errors following the initial steering transient associated with initiation of the stage 2 closed-loop guidance. This misalignment effect was again observed near MECO when the main engines were throttled to their minimum thrust level (65%) just prior to MECO. The structural relaxation during the engine shutdown left the vehicle with a small residual rate in pitch that the RCS quickly nulled as control was transferred from the ascent TVC to the Trans DAP RCS thrusters following MECO. There was no discernable bending activity observable in the stage 2 autopilot parameters and the propellant slosh activity was barely noticable in the rate gyro data. A small amount of oscillation at the slosh frequency was anticipated due to rate gyro quantization and TVC nonlinearities.

Reconstruction of the vehicle performance indicated that the MPS thrust levels were very close to predictions, with some trend toward increasing thrust noted on engines 1 and 3. This was found to be due to the temperature effects on the sensed engine chamber pressure used by the engine control computers to maintain a constant thrust level. Overall vehicle $I_{sp}$ was approximately 2 s less than predicted.

The GN&C system steered the vehicle to a MECO state that was well within the predicted accuracy at cutoff. Inertial velocity was only 1.4 ft/s low, which is less than the average error expected due to the 25 Hz computation rate for MECO predictions.

Following MECO, the main engines are commanded to their full-down position limit for the dumping of the main propulsion system's residual propellants, an operation scheduled concurrently with the first OMS burn. Following completion of the burn and dump, the MPS engines are commanded to a stow position for the remainder of the mission. Just prior to ET separation, an unexpected RCS thruster firing was noticed that was due to transient pitch rate exceedance of the Trans DAP deadbands. The software processing rate for TVC actuator commands was reduced from 25 to 1.0 Hz following MECO, resulting in the engines being slewed to their dump and stow positions in increments of 1 deg. A pitch axis bending oscillation of about 0.5 deg/s peak-to-peak at 4 Hz was noted during these periods of engine slew. Fortunately, the Trans DAP rate limits were large enough to avoid serious RCS interactions, but the extra jet firing used an additional 10 lb of RCS propellant. A software change is planned to correct this problem in future flights.

The right OMS engine pitch actuator froze at the null position midway through the OMS-2 circularization burn. During the burn the engines were well trimmed and the OMS actuator malfunction caused no significant transient. The actuator performed sluggishly during slew checks following OMS-2 and the secondary drive motor in the actuator was used for the remainder of the mission. Postflight troubleshooting isolated the problem to insufficient rotor/stator clearances to accomodate the dynamic deflections encountered. The actuator was replaced for STS-2.

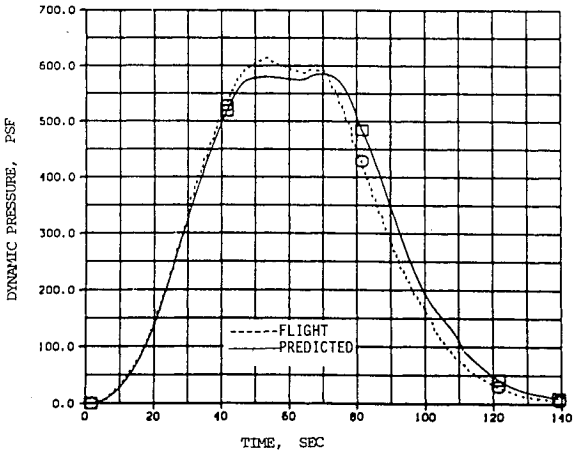


Fig. 7 STS-1 dynamic pressure.

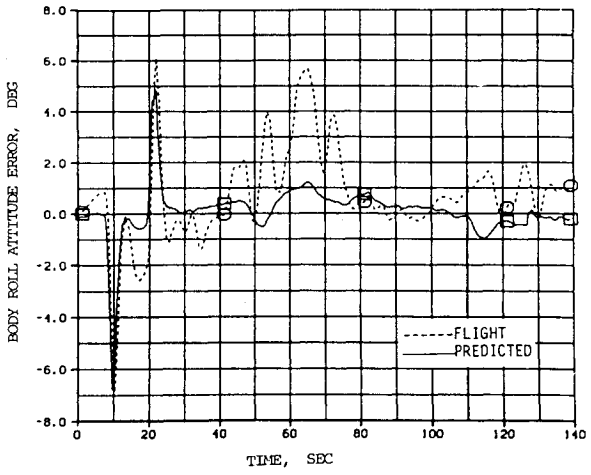


Fig. 9 STS-2 roll attitude error.

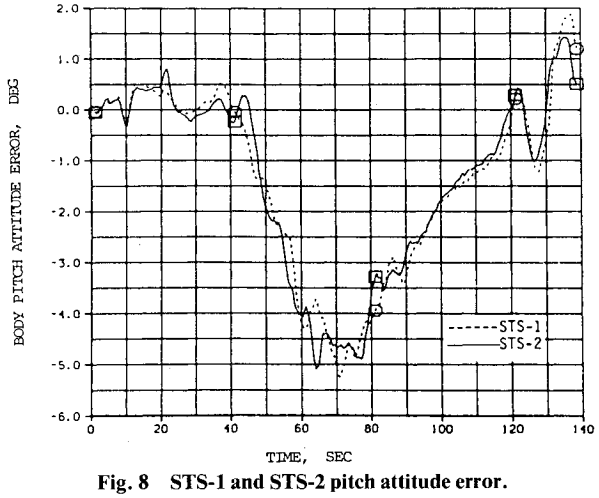


Fig. 8 STS-1 and STS-2 pitch attitude error.

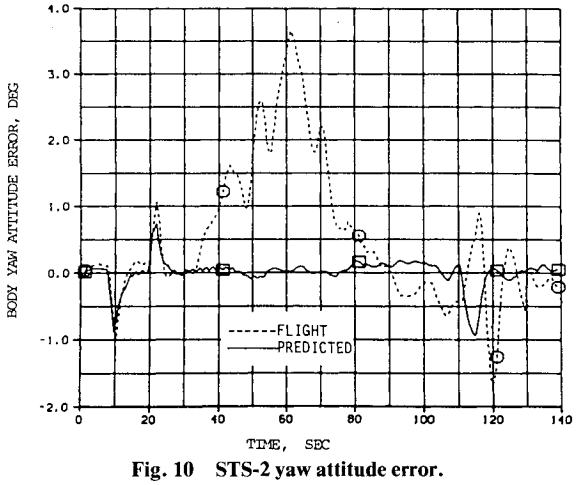


Fig. 10 STS-2 yaw attitude error.

Adequate redundancy exists in each actuator should the failure occur again. Further redundancy exists in the OMS/RCS pods themselves, as the RCS thrusters will correct for any significantly offset thrust vector. Design changes are in progress for the OMS actuators to be installed on subsequent vehicles.

## GN&C Changes for the Second Flight

As a result of the excellent performance of the GN&C system on STS-1, only minimal software changes were required for the second test flight—specifically, a small compensation for the lofting phenomenon observed in first stage. The performance predictions for STS-2 when the design trajectory was evaluated using reconstructed ascent aero, propulsion predictions, and seasonal environmental effects indicated a poor payload performance margin. To partially compensate for the first-stage lofting, the open-loop first-stage attitude profile was adjusted to compensate for half of the flight path angle error at the SRB staging. The orbital inclination and targeted orbital altitude were decreased somewhat to provide an increased performance margin as STS-2 carried an additional 10,000 lb of payload compared to STS-1. In addition, the trajectory profile scribe lines provided on the cockpit CRT displays to allow crew monitoring of trajectory performance were adjusted based on the aerodynamic/induced lofting observed on STS-2.

## Results of the Second Flight

Launch of STS-2, the second Shuttle test flight, occurred on Nov. 12, 1981. GN&C system performance and response compared well with that observed on STS-1. The launch facility clearance margins were again determined to be near nominal, this time with the assistance of data provided by improved engineering camera coverage. The aerodynamic characteristics of STS-1 first-stage flight were reconfirmed as the pitch attitude error again grew to −5.2 deg (see Fig. 8). The vehicle encountered a significant amount of crosswind in the altitude region of 35,000 ft that produced the roll and yaw attitude errors shown in Figs. 9 and 10. Note also in Fig. 10 the yaw attitude error in the region of 115-120 s, which was due to a slight SRB mismatch as the SRB thrust is tailing off near the end of the first stage.

Close examination of redundant rate gyro data for the STS-2 first stage revealed the existence of a small amount of pitch angular misalignment of all three left-hand SRB rate gyro assemblies. During the roll maneuver following tower clearance, the selected left SRB yaw rate signal was approximately 0.2 deg/s less than either the selected signal from the right-hand SRB or the Orbiter rate gyros. During the remainder of the first stage, there was no disagreement, thus indicating a cross coupling of the roll rate into the sensed yaw rate signal rather than a bias from null. Postflight trajectory simulations incorporating a postulated 1.2 deg angular misalignment in pitch of the sensors in question produce simulated dynamic body rate histories that agree extremely well with the flight response. Although the total error was small as seen by the autopilot (the selected left and right SRB rate signals are averaged), the alignment error is slightly larger than allowed by specification. Following SRB recovery, gyro alignment checks confirmed the suspected alignment error

**Table 2 Stage 2 MPS thrust misalignment**

| Pitch = deg | Yaw = deg |
|---|---|
| 1 = −0.40 | 1 = +0.1 |
| 2 = −0.25 | 2 = −0.3 |
| 3 = −1.45 | 3 = +0.8 |

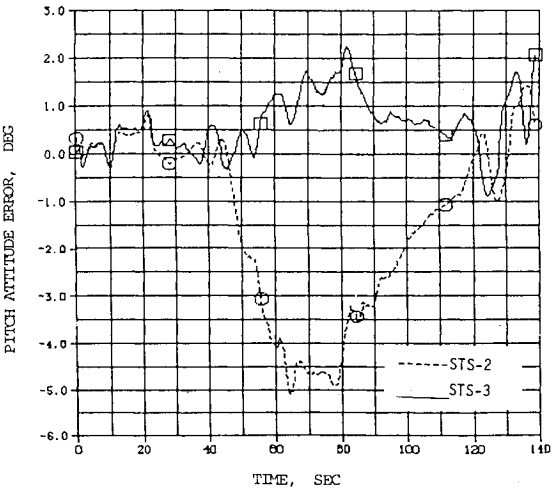


**Fig. 11 Comparison of pitch attitude error.**

and appropriate steps have been taken to assure proper installation on future missions.

Stage 2 GN&C transient and steady-state response was comparable to STS-1. Several autopilot software parameters from the GPS were included in the variable downlist, including the autotrim integration signals. Postflight reconstruction of stage 2 attitude error, autotrim integration, and TVC actuator command histories reconfirmed the level of Orbiter thrust vector misalignment observed on STS-1. The estimated alignments are shown in Table 2.

Reconstruction of vehicle performance again showed vehicle $I_{sp}$ to be 2 s below expected. For STS-2, the engine's chamber pressure transducer harnesses received additional insulation and the thrust trending observed on STS-1 was eliminated. A minor change in the engine controller software caused the main engines to operate very close to the nominal 6.0/1.0 mixture ratio compared to the 6.03/1.0 observed on STS-1.

MECO accuracy was again exellent on STS-2 and overall GN&C performance for ascent was as predicted.

## Results of the Third Flight

First-stage aerodynamic characteristics extracted from the flight data from STS-1 and STS-2 were used as the design data base to develop stage 1 steering, SRB trim, and reference normal acceleration profiles for flight 3.

STS-3 was launched on March 22, 1982 and the GN&C system again performed nominally throughout ascent. The aerodynamically induced lofting experienced on the first two flights was successfully eliminated by using aero characteristics extracted from flight data to develop trim tables for the flight software. A comparison of the pitch attitude error between STS-2 and STS-3 is shown in Fig. 11. Note that for STS-3 the pitch error was somewhat positive, due to a headwind component and to an SRB burn rate that was approximately 2% less than preflight predictions.

Second-state performance and response agree well with preflight predictions using the 2 s low specific impulse for the main engines observed on flights 1 and 2. Attitude errors were small and again reflected the MPS thrust misalignment observed on the earlier flights.

The only subsystem malfunction seen in ascent was a rapid rise of the No. 3 auxiliary power units gearbox oil temperature, which exceeded the redline prior to MECO. At the request of Mission Control, the crew shut down the unit approximately 25 s prior to MECO, resulting in a loss of hydraulic supply pressure to the No. 3 main engine. The engine throttle was locked at approximately 80% and shutdown at MECO was achieved using the backup pneumatic valve closure system. The slight thrust imbalance during MECO tailoff produced small body rates that the RCS jets easily controlled following activitation. The off-nominal thrust situation late in stage 2 had little effect on MECO accuracy as the cutoff velocity error was less than 1.0 ft per second.

## Conclusions

In summary the ascent GN&C system performed in an excellent fashion on the first three Space Shuttle test flights. Data gathered on subsystem response is being used to improve the analytical mathematical models in order to provide more accurate predictions of vehicle behavior for future missions. Minor modifications to hardware and software will continue as increased flight capabilities are added as a result of the expanding data base obtained in the Space Shuttle flight test program.

## References

[1] Glandorf, D.R., "Analysis and Gain Synthesis Techniques for the Space Shuttle Ascent Flight Control System," Vol. I, NASA JSC-16724, June 1980.

[2] "STS-1 Orbiter Final Mission Report," NASA JSC-17378, Aug. 1981.

[3] "STS-1 Integrated Systems Evaluation Final Report," NASA JSC-17508, Aug. 1981.